



A GENUINELY MULTIDISCIPLINARY JOURNAL

CHEMPLUSCHEM

CENTERING ON CHEMISTRY

Accepted Article

Title: Protonated Poly(ethylene imine)-Coated Silica Nanoparticles for Promoting Hydrogen Generation from NaBH₄ Hydrolysis

Authors: Lijing Yang, Xiaoshan Huang, Jiapeng Zhang, and Hua Dong

This manuscript has been accepted after peer review and appears as an Accepted Article online prior to editing, proofing, and formal publication of the final Version of Record (VoR). This work is currently citable by using the Digital Object Identifier (DOI) given below. The VoR will be published online in Early View as soon as possible and may be different to this Accepted Article as a result of editing. Readers should obtain the VoR from the journal website shown below when it is published to ensure accuracy of information. The authors are responsible for the content of this Accepted Article.

To be cited as: *ChemPlusChem* 10.1002/cplu.201900609

Link to VoR: <http://dx.doi.org/10.1002/cplu.201900609>

WILEY-VCH

www.chempluschem.org

A Journal of



Protonated Poly(ethylene imine)-Coated Silica Nanoparticles for Promoting Hydrogen Generation from NaBH₄ Hydrolysis

Lijing Yang, Xiaoshan Huang, Jiapeng Zhang, and Dr. Hua Dong*

Abstract: Due to the advantages including high activity, low cost, and environmental friendliness, nonmetal catalysts are attracting more and more attention. In this work, a nonmetal catalyst for NaBH₄ hydrolysis is fabricated through covalent modification of silica nanoparticles with protonated poly(ethylene imine). The successful fabrication of the catalyst is verified with transmission electron microscopy, thermogravimetric analysis, and Fourier transform infrared spectroscopy. The fabricated catalyst shows excellent activity in catalyzing NaBH₄ hydrolysis reactions. The hydrolysis of 15 mg NaBH₄ catalyzed by 50 mg catalyst could provide a hydrogen generation rate as high as 117.53 mL min⁻¹ g_{cat}⁻¹ at 20 °C. Although the catalytic activity could decrease after use, it could be restored easily by regenerating in acetic acid solution.

Introduction

The increasing global energy consumption has brought about a series of problems, including fossil fuel depletion and environmental pollution. It makes the development of renewable energy source ever more essential than before.^[1,2] It is well-known that hydrogen (H₂) is one of the most important alternatives to conventional fossil fuels because of its high energy density and clean emission.^[3] In the last years, a vast number of materials in which hydrogen can be stored physically or chemically have been developed.^[4] Sodium borohydride (NaBH₄),^[5-7] ammonia borane (NH₃BH₃)^[8-9] and hydrazine borane (N₂H₄BH₃)^[10] are some of the representatives. NaBH₄ is an attractive chemical hydride which can release 4 equivalents H₂ while hydrolyzing. Nevertheless, the NaBH₄ self-hydrolysis without a catalyst is intolerably slow.^[7,11] Thus, suitable catalysts which can endow NaBH₄ hydrolysis a decent rate are highly demanded.

In the last years, varieties of metal catalysts for promoting NaBH₄ hydrolysis, including Ru,^[12-15] Pd,^[16] Ag,^[17] Mn,^[18] Co,^[19-29] Ni,^[20,30-32] and complexes of them,^[33-42] have been extensively investigated. Although these metal catalysts have shown excellent catalytic performance in NaBH₄ hydrolysis, their high cost and complicated fabrication are obstacles on their way to practical applications. Furthermore, due to the aggregation of the metal nanoparticles in the reaction, the catalytic activity of the metal catalysts often cannot last.^[13,14] Therefore, nonmetal

catalysts for NaBH₄ hydrolysis or alcoholysis have recently attracted more and more attention. For example, ammonium-based catalysts, reported for the first time by Lu et al.,^[43] showed very high catalytic activity for KBH₄ hydrolysis. Furthermore, Saka et al. studied the catalytic activity of hydrochloric acid and acetic acid on NaBH₄ methanolysis,^[44] as well as the catalytic activity of phosphoric acid on KBH₄ hydrolysis.^[45] Asiri and Khan et al. studied chitosan coated cotton fiber which showed high activity and good reusability in NaBH₄ methanolysis.^[46] Especially, Sahiner's group has recently made great contributions to this topic. Based on poly(4-vinyl pyridine) particles,^[47] silica particles,^[48] poly(ethylene imine) microgels,^[49] carbon spheres,^[50] carbon nanotubes,^[51] etc., they developed kinds of catalysts with good catalytic performance for NaBH₄ methanolysis. These reports proved that nonmetal catalysts had amazing catalytic performance. Moreover, compared with their metal counterparts, these nonmetal catalysts also showed advantages on the aspects of low cost and environmental friendliness.^[43,46-48]

Herein, we report a nonmetal catalyst for NaBH₄ hydrolysis, which is composed of SiO₂ nanoparticles covalently modified with protonated poly(ethylene imine) (SiO₂@H⁺PEI) (Figure 1). The fabrication of the catalyst was realized by simple surface modification of SiO₂ nanoparticles. The characterizations with transmission electron microscopy (TEM), thermogravimetric (TG) analysis, and Fourier transform infrared (FT-IR) spectroscopy have verified the successful fabrication of the catalyst. H₂ generation experiments showed that the fabricated SiO₂@H⁺PEI catalyst had excellent performance on promoting NaBH₄ hydrolysis. Although the activity of the catalyst decreased in cycle use, it can be restored after the catalyst was regenerated in acetic acid solution. This fabricated SiO₂@H⁺PEI catalyst could provide a promising choice for efficiently promoting NaBH₄ hydrolysis in a cheap way.

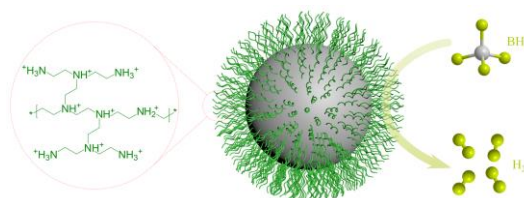


Figure 1. Schematic illustration of H₂ generation from NaBH₄ hydrolysis catalyzed by SiO₂@H⁺PEI.

Results and Discussion

Figure S1 has shown the SEM images of SiO₂ nanoparticles and SiO₂@H⁺PEI catalyst. It can be clearly seen that SiO₂

L. Yang, X. Huang, J. Zhang, Dr. H. Dong
College of Materials and Chemistry & Chemical Engineering,
Chengdu University of Technology, Chengdu 610059, China
E-mail: donghua@iccas.ac.cn

Supporting information for this article is given via a link at the end of the document. ((Please delete this text if not appropriate))

nanoparticles formed loose spongy aggregation (Figure S1a), while the fabricated $\text{SiO}_2@H^+PEI$ catalyst was relatively more compact (Figure S1b). As shown in TEM images in Figure 2, the aggregates of both SiO_2 and $\text{SiO}_2@H^+PEI$ could be easily separated to small nanoparticles. And the morphology of $\text{SiO}_2@H^+PEI$ was not significantly different from that of SiO_2 nanoparticles. Compared with SiO_2 nanoparticles, $\text{SiO}_2@H^+PEI$ had almost the same size, but with aggregates slightly formed. The size of the formed aggregates was around tens of nanometers. Furthermore, the composition of nanoparticles was confirmed with element mapping. For SiO_2 (Figure 3a), it could be clearly observed that there were distinct Si and O signals, while no significant C signal could be observed. In contrast, for $\text{SiO}_2@H^+PEI$ (Figure 3b), C signal could be clearly observed as well as Si and O signals. It means that the protonated PEI chains had been successfully grafted on the surface of SiO_2 in $\text{SiO}_2@H^+PEI$ catalyst.

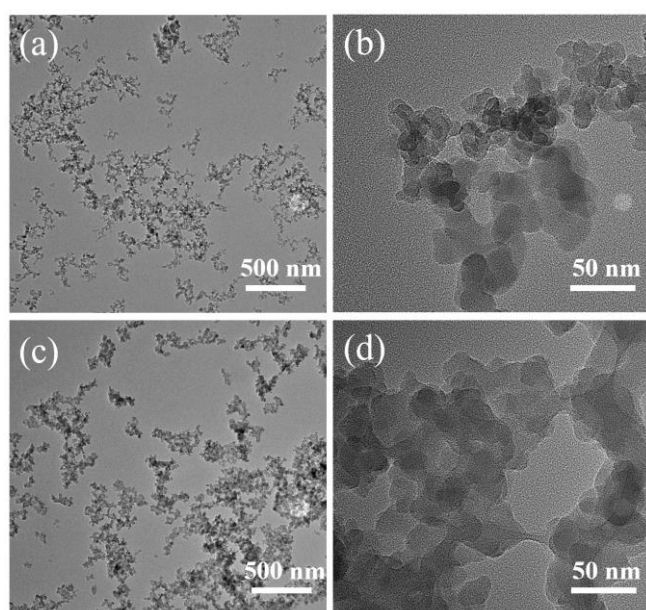


Figure 2. TEM images of SiO_2 (a, b) and $\text{SiO}_2@H^+PEI$ (c, d). Slight aggregation could be observed after modification (c, d). The size of $\text{SiO}_2@H^+PEI$ is still around tens of nanometers.

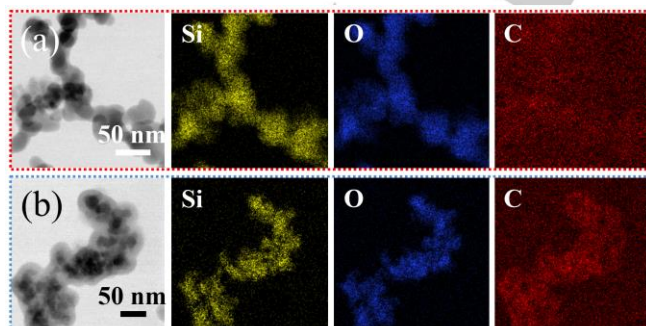


Figure 3. Element mapping of SiO_2 (a) and $\text{SiO}_2@H^+PEI$ (b). Distinct Si and O signals can be seen for both SiO_2 and $\text{SiO}_2@H^+PEI$. However, C signal can only be seen for $\text{SiO}_2@H^+PEI$. No significant C signal can be observed for

SiO_2 . It indicates that the polymer chains have been successfully grafted onto the surface of SiO_2 in $\text{SiO}_2@H^+PEI$ catalyst.

The change of surface composition after the modification was further analyzed with XPS. As shown in Figure S2a and Figure S2c, Si 2p spectra was almost the same for both unmodified SiO_2 and $\text{SiO}_2@H^+PEI$. However, the N 1s peak, which could not be observed for unmodified SiO_2 (Figure S2b), appeared in $\text{SiO}_2@H^+PEI$ (Figure S2d), indicating the success of modification.

Figure 4 shows the thermogravimetric analysis results of SiO_2 and $\text{SiO}_2@H^+PEI$. The dark yellow curve shows that there was around 30% weight loss when $\text{SiO}_2@H^+PEI$ was heated to 160 °C, which should be caused by the elimination of acetic acid released from the decomposition of PEI acetate. Subsequently, a distinct weight loss was observed between 310 °C and 380 °C, which could be attributed to the decomposition of PEI residual on the surface of SiO_2 . The weight of the sample gradually tended to be constant when temperature was above 400 °C, indicating total decomposition of organic components. When the temperature was 800 °C, there was only 35.78% of the initial weight left in the sample. As a control, the unmodified SiO_2 sample was tested under the same condition. The result (light blue curve) showed that there was 96.28% of the initial weight left after being heated to 800 °C. The big difference between the weight losses of the two samples indicates that plenty of protonated PEI had been successfully anchored on the surface of SiO_2 to form $\text{SiO}_2@H^+PEI$ catalyst.

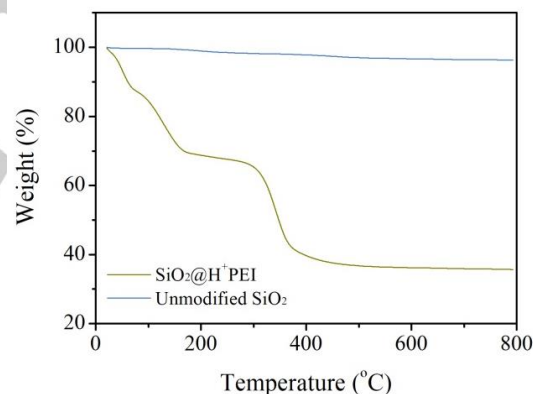


Figure 4. Thermogravimetric curves of SiO_2 (light blue curve) and $\text{SiO}_2@H^+PEI$ (dark green curve). The large weight loss of $\text{SiO}_2@H^+PEI$ indicates that there are considerable organic components in $\text{SiO}_2@H^+PEI$.

To confirm the success of each step of the modification (Figure S3), FT-IR tests were carried out for the related products. The results were shown in Figure 5. The modification of amino groups on the surface of SiO_2 did not change the IR spectra a lot (Figure 5b). However, when it was further modified with hexanedioic acid, peaks of carboxylic groups at 1740 cm^{-1} and 1211 cm^{-1} , peak of hydroxyl groups of carboxylic acid at 896 cm^{-1} , and peaks of methylene groups at 2951 cm^{-1} and 2880 cm^{-1} appeared (Figure 5c). The following PEI modification brought about the disappearance of characteristic peaks of hexanedioic acid modified SiO_2 nanoparticles (1740 cm^{-1} , 1211 cm^{-1} , and 896 cm^{-1}) (Figure 5d), which means the carboxylic groups on the surface fully reacted with amino groups in PEI. After the last modification step, the peak at 1417 cm^{-1} which was from

carboxylate formed from amino groups in PEI and carboxylic groups in acetic acid appeared (Figure 5e). Furthermore, compared with SiO_2 modified with hexanedioic acid (Figure 5c), the final product $\text{SiO}_2@H^+PEI$ did not have the peak of hydroxyl groups in carboxylic acid at 896 cm^{-1} . It indicates that all acetic acid molecules formed carboxylate in the $\text{SiO}_2@H^+PEI$ catalyst, and that there were no free carboxylic groups.

From the analysis above, it can be concluded that the changes of IR spectra from the products of each modification step have clearly verified the success of the fabrication of the $\text{SiO}_2@H^+PEI$ catalyst.

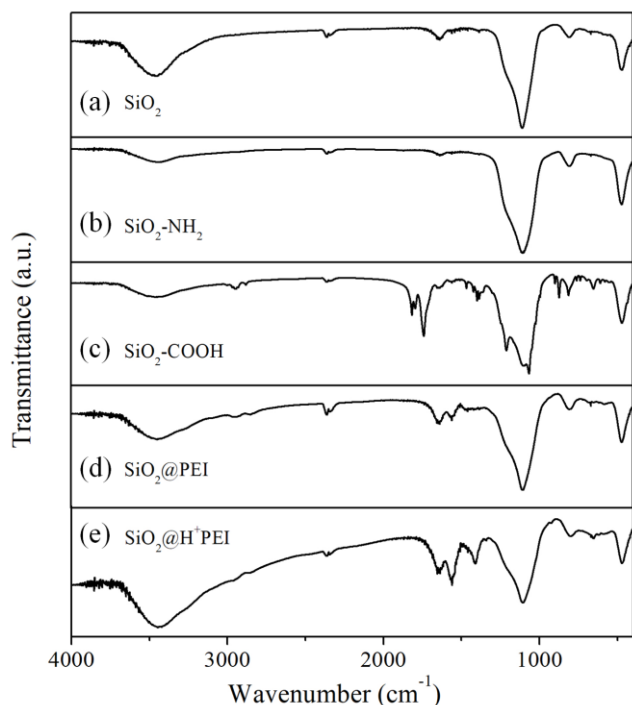


Figure 5. FT-IR spectra of the products of each modification step. (a) SiO_2 : Unmodified SiO_2 ; (b) $\text{SiO}_2\text{-NH}_2$: Product of SiO_2 modified with (3-aminopropyl)triethoxysilane; (c) $\text{SiO}_2\text{-COOH}$: Product from $\text{SiO}_2\text{-NH}_2$ further modified with hexanedioic acid; (d) $\text{SiO}_2@PEI$: Product from $\text{SiO}_2\text{-COOH}$ modified with poly(ethylene imine); (e) $\text{SiO}_2@H^+PEI$: Product from $\text{SiO}_2@PEI$ protonated with acetic acid. The appearance and disappearance of related characteristic peaks after each modification step have clearly verified the successful fabrication of $\text{SiO}_2@H^+PEI$ catalyst.

The catalytic performance of the $\text{SiO}_2@H^+PEI$ catalyst was evaluated with the rate of H_2 generation from catalyzed NaBH_4 hydrolysis. Different from metal catalysts which often give a nearly constant H_2 generation rate in the whole process of NaBH_4 hydrolysis or alcoholysis,^[14,52-54] nonmetal catalysts normally give gradually decreasing H_2 generation rate,^[46,48,50] making the calculation of H_2 generation rate complicated. To make the evaluation of catalytic activity of the catalysts easier, the average H_2 generation rate per gram for producing the first half amount of H_2 ($\text{HG}_{1/2}$ rate) was measured for each reaction.

As shown in Figure 6a, the fabricated $\text{SiO}_2@H^+PEI$ catalyst had shown excellent activity for NaBH_4 hydrolysis. It powerfully promoted H_2 generation at the beginning of the reactions, while due to the neutralization effect caused by the accumulation of

NaBO_2 in the solution, the H_2 generation rate gradually slowed down as the reactions progressed. Nevertheless, the $\text{HG}_{1/2}$ rate of NaBH_4 hydrolysis catalyzed by $\text{SiO}_2@H^+PEI$ was as high as $117.53\text{ mL min}^{-1}\text{ g}_{\text{cat}}^{-1}$. The unmodified SiO_2 was used as control, and the $\text{HG}_{1/2}$ rate was $3.19\text{ mL min}^{-1}\text{ g}_{\text{cat}}^{-1}$, which was slightly higher than that of the reactions uncatalyzed (1.87 mL min^{-1}) under the same conditions (Figure 6b).

To prove that it was the protonation of PEI that had endowed the catalyst with the activity, unprotonated $\text{SiO}_2@PEI$ and protonated $\text{SiO}_2@H^+PEI$ but washed with saturated NaHCO_3 solution were tested as well. As shown in Figure 6, the H_2 generation experiments catalyzed by unprotonated $\text{SiO}_2@PEI$ catalyst (red circles in Figure 6a) had a $\text{HG}_{1/2}$ rate of $4.41\text{ mL min}^{-1}\text{ g}_{\text{cat}}^{-1}$, which was similar to the rate of reactions catalyzed by unmodified SiO_2 , and much slower than that of $\text{SiO}_2@H^+PEI$ catalyzed reactions. Furthermore, after washed with adequate NaHCO_3 solution, the protonated $\text{SiO}_2@H^+PEI$ lost the protons and showed an even slower $\text{HG}_{1/2}$ rate of $1.74\text{ mL min}^{-1}\text{ g}_{\text{cat}}^{-1}$ in H_2 generation experiments. It means that the protonation of PEI was indispensable for the high activity of the catalyst, and the further deprotonation could vanish the catalytic activity.

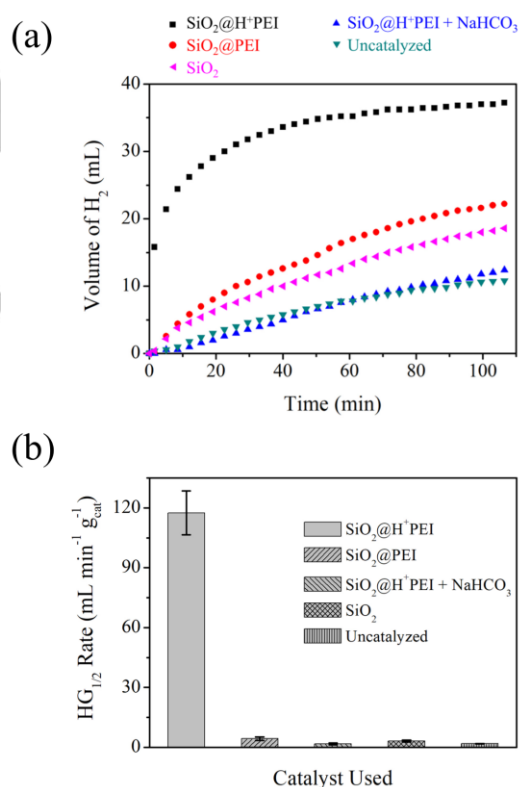


Figure 6. H_2 generation from NaBH_4 hydrolysis catalyzed by different catalysts. (a) Plots of H_2 volume (mL) versus time (min) for reactions catalyzed by different catalysts; (b) H_2 generation rate per gram catalyst for producing the first half amount of H_2 ($\text{HG}_{1/2}$ rate) for different catalysts. The very high $\text{HG}_{1/2}$ rate of reaction catalyzed by $\text{SiO}_2@H^+PEI$ indicates its high catalytic activity. Experiment conditions: 50 g reaction mixture, 50 mg catalysts, 15 mg NaBH_4 , $20\text{ }^\circ\text{C}$.

According to the analysis of Lu et al.,^[43] the pathway of borohydride hydrolysis catalyzed by ammonium catalysts could be divided into several barrierless and low-barrier elementary steps. The supposed mechanism explained the high activity of ammonium catalysts in catalyzing borohydride hydrolysis. Therefore, a similar mechanism as shown in Figure 7 could be proposed for the NaBH₄ hydrolysis catalyzed by SiO₂@H⁺PEI. The first step of the reaction ($\bullet\text{-NH}_3^+ + \text{BH}_4^- \rightarrow \bullet\text{-NH}_2 + \text{BH}_3 + \text{H}_2$) is a barrierless reaction, and the resulted intermediate BH₃ is very active for the following steps, which makes the whole hydrolysis reaction very fast.

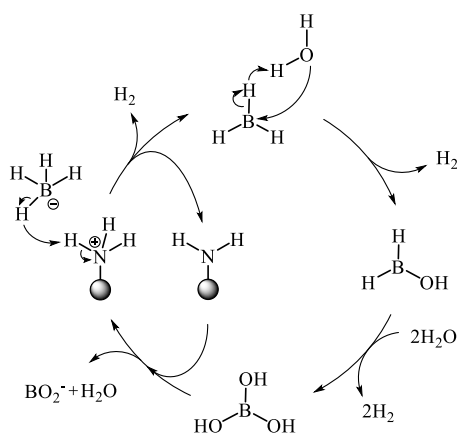


Figure 7. Proposed mechanism of NaBH₄ hydrolysis catalyzed by SiO₂@H⁺PEI.

Figure S4 shows the effect of NaBH₄ amount on the rate of hydrolysis reactions. The H₂ generation plots in Figure S4a demonstrated different plateaus, showing the final volume of H₂ produced increased with the increasing of NaBH₄ amount. From Figure S4b, it could be found that the final amount of produced H₂ increased linearly with the increasing of NaBH₄ amount. Figure S4c shows that the HG_{1/2} rate firstly decreased linearly from 426.38 mL min⁻¹ g_{cat}⁻¹ to 117.52 mL min⁻¹ g_{cat}⁻¹ while the amount of NaBH₄ used increased from 5 mg to 15 mg. However, while the amount of NaBH₄ used was further increased from 15 mg to 25 mg, the HG_{1/2} rate did not change significantly. These results mean that when NaBH₄ concentration was low, the H₂ generation rate was decided by NaBH₄ concentration, while when NaBH₄ concentration was high, the H₂ generation rate was much less related with the change of NaBH₄ concentration. Nevertheless, in the range of our experiments, the changing of NaBH₄ concentration had no distinct effect on yield of H₂ in the catalyzed NaBH₄ hydrolysis.

Temperature is an important factor which affects the rate of NaBH₄ hydrolysis drastically. To investigate the temperature effect, the H₂ generation reactions were carried out at 20 °C, 30 °C, 40 °C, and 50 °C. As shown in Figure 8, the H₂ generation rate increased dramatically with the increasing of reaction temperature. The HG_{1/2} rate at 20 °C was 117.52 mL min⁻¹ g_{cat}⁻¹, while at 50 °C it was 419.80 mL min⁻¹ g_{cat}⁻¹, with 3.6 times increasing (Figure S5). With the data from H₂ generation reactions at different temperatures, the activation energy (E_a) of the catalyzed reactions was calculated according to Arrhenius equation:

$$\ln k = \ln A - E_a/RT \quad (1)$$

where T represents the temperature of H₂ generation reaction in Kelvin (K), k represents the corresponding rate constant of the reactions, R represents the gas constant, and A represents pre-exponential factor. The E_a of the catalyzed reactions was calculated at about 32.01 kJ mol⁻¹ (Figure 8b). This value is comparable with or even less than the activation energy of many other NaBH₄ hydrolysis reactions catalyzed by metal catalysts (32.66 kJ mol⁻¹ for hydrogel-Ni composites,^[32] 36.4 kJ mol⁻¹ for Ru/ZIF-67,^[13] 40.7 kJ mol⁻¹ for AuCo/Cu,^[34] 49.2 kJ mol⁻¹ for Co/Fe₃O₄@C,^[27] 56.9 kJ mol⁻¹ for Co@C composites,^[28] etc.). It indicates that the fabricated SiO₂@H⁺PEI catalyst has great potential in practical H₂ production applications.

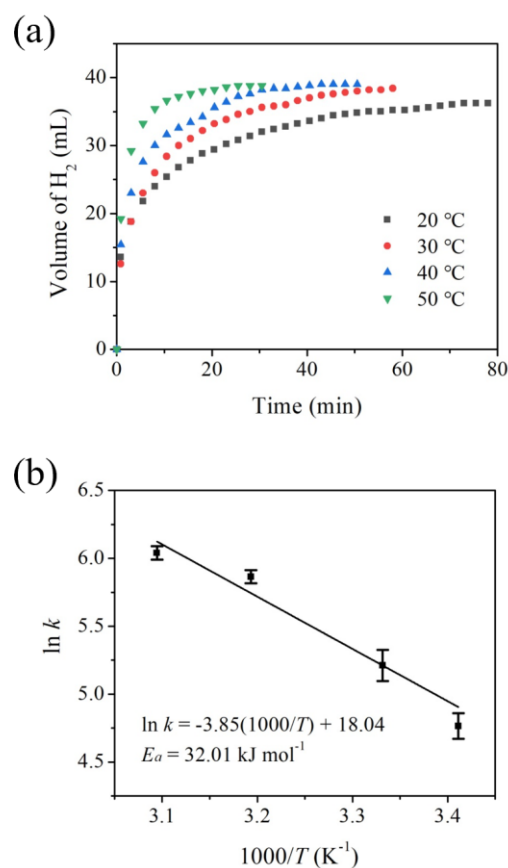


Figure 8. H₂ generation from NaBH₄ hydrolysis catalyzed by SiO₂@H⁺PEI at different reaction temperature. (a) Plots of H₂ volume (mL) versus time (min) for reactions at different temperature; (b) Arrhenius plot for NaBH₄ hydrolysis catalyzed by SiO₂@H⁺PEI. Experiment conditions: 50 g reaction mixture, 50 mg SiO₂@H⁺PEI, 15 mg NaBH₄.

To confirm the reusability of the catalyst, the catalytic activity of used catalyst was tested. It could be seen, in Figure 9a, that the catalytic activity of SiO₂@H⁺PEI dropped off sharply after used for once. As mentioned previously, the catalytic activity of SiO₂@H⁺PEI came from the protonation of PEI. When it was used in NaBH₄ hydrolysis, the byproduct NaBO₂ from the reaction neutralized protons of SiO₂@H⁺PEI, resulting in sharp decreasing of the activity. However, when the neutralized

catalyst was regenerated by being immersed in aqueous acetic acid solution and dried in vacuum again, it could be protonated again and the dropped activity could be restored. The H_2 generation experiment results shown in Figure 9b have obviously demonstrated that the regenerated catalysts had almost the same activity as the original one, even after being used for several cycles. These results indicated that $SiO_2@H^+PEI$ had excellent reusability in catalyzing $NaBH_4$ hydrolysis.

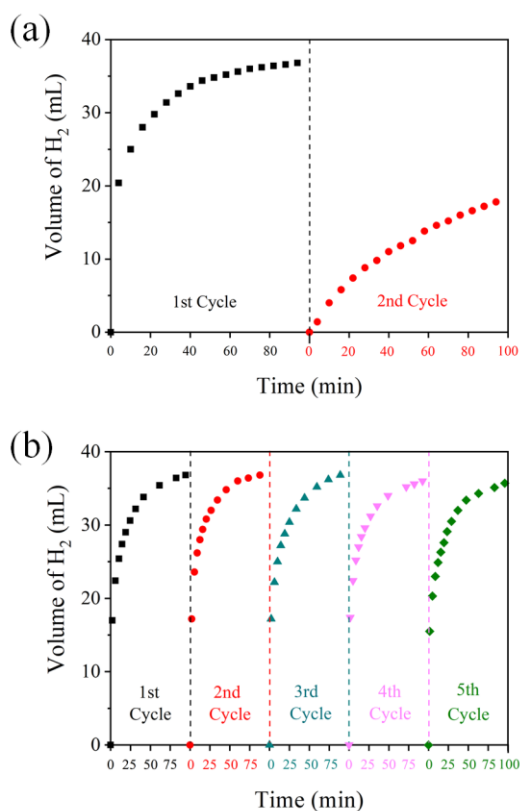


Figure 9. The reusability of $SiO_2@H^+PEI$ catalyst. (a) The activity of $SiO_2@H^+PEI$ catalyst decreases distinctly after used for once. (b) The catalytic activity of used $SiO_2@H^+PEI$ catalyst can be restored after regenerated in acetic acid solution. The reactions catalyzed by the regenerated catalysts show similar rate to the reactions catalyzed by the original $SiO_2@H^+PEI$ catalyst. Experiment conditions: 50 g reaction mixture, 15 mg $NaBH_4$, 50 mg $SiO_2@H^+PEI$, 20 °C.

In addition to hydrolysis, methanolysis of $NaBH_4$ is also very important. Generally, the rate of $NaBH_4$ methanolysis is much faster than its hydrolysis rate under the same conditions. As shown in Figure S6, for the methanolysis reactions at 20, 25, and 30 °C, it took 8.0, 4.8, and 2.8 min respectively to produce 259 mL H_2 , which were comparable with the results reported in previous studies.^[55-58]

Conclusions

In summary, by modifying SiO_2 nanoparticles with protonated PEI, a novel nonmetal catalyst for $NaBH_4$ hydrolysis, $SiO_2@H^+PEI$, was fabricated. TEM with element mapping, TG analysis, and FT-IR have verified the successful fabrication of the catalyst. The obtained catalyst showed excellent catalytic activity and good reusability for promoting $NaBH_4$ hydrolysis, providing a promising choice for H_2 production applications.

Experimental Section

Catalyst preparation

As illustrated in Figure S3, the catalyst was prepared with a procedure as following:

(1) SiO_2 nanoparticles were dispersed in toluene, into which (3-aminopropyl)triethoxysilane was added. The mixture was stirred at 80 °C overnight. Then the solid was collected, and washed thoroughly with toluene and ethanol sequentially to obtain amino modified SiO_2 nanoparticles.

(2) After drying in vacuum, the amino modified SiO_2 nanoparticles were dispersed in an aqueous solution of EDC, NHS and hexanedioic acid to form a mixture with $m_{SiO_2}:m_{EDC}:m_{NHS}:m_{HA}$ 2:2:1:1. After the mixture was stirred overnight at 25 °C, the solid was collected, washed thoroughly with water to obtain carboxyl modified SiO_2 nanoparticles.

(3) The carboxyl modified SiO_2 nanoparticles were dispersed in an aqueous solution of EDC, NHS and PEI to form a mixture with $m_{SiO_2}:m_{EDC}:m_{NHS}:m_{PEI}$ 2:2:1:10, which was then stirred overnight at 25 °C. The solid was collected by centrifuging, and washed thoroughly with water.

(4) The PEI modified SiO_2 nanoparticles obtained from the previous step were immersed in an aqueous solution of acetic acid (10%). The mixture was stirred at 25 °C for 1 hour. After the solid was collected by centrifuging, it was dried at 80 °C in vacuum to obtain $SiO_2@H^+PEI$ in powder.

Catalyst characterization

SEM investigation was carried out on an SEM machine (MERLIN Compact, Zeiss). TEM investigation and element mapping were carried out on a TEM machine (Tecnai G2 F20, FEI). XPS analysis was carried out on an x-ray photoelectron spectrometer (EscaLab 250Xi, ThermoFisher). TG analysis was carried out in nitrogen on a TG analyzer (TA Instruments, Q600). FT-IR was carried out using an FT-IR machine (ThermoFisher, Nicolet iS10).

Catalyst performance evaluation

The experiments of H_2 generation from $NaBH_4$ hydrolysis were carried out to evaluate the catalytic activity of the obtained $SiO_2@H^+PEI$. Figure S7 shows an illustration of the experiment set-up. In each experiment, the flask was charged with 40 g water dispersion of catalysts and then sealed. 10 g aqueous $NaBH_4$ solution was injected into the flask to form 50 g reaction mixture. After the produced H_2 was washed with anhydrous $CaCl_2$, it was collected and measured with a glass burette.

The $NaBH_4$ methanolysis experiments were carried out in the same experiment set-up. In each experiment, the flask was sealed after 100 mg $NaBH_4$, 50 mg $SiO_2@H^+PEI$ were added, and then 20 mL methanol was injected into the flask to initiate the methanolysis reactions.

Acknowledgements

This work was supported by Chengdu University of Technology.

Keywords: heterogeneous catalysis • hydrogen generation • nanoparticles • polymers • silica

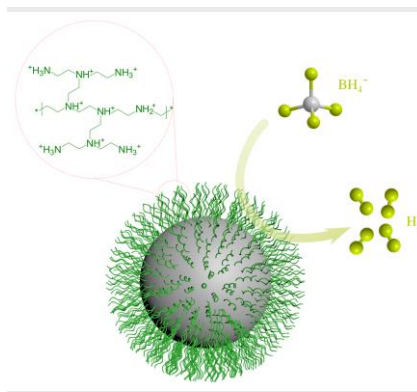
- [1] S. J. Wang, G. D. Li, C. L. Fang, *Renew. Sust. Energy Rev.* **2018**, *81*, 2144-2159.
- [2] T. Hisatomi, K. Domen, *Nat. Catal.* **2019**, *2*, 387-399.
- [3] D. Parra, L. Valverde, F. J. Pino, M. K. Patel, *Renew. Sust. Energy Rev.* **2019**, *101*, 279-294.
- [4] K. Wang, Z. X. Pan, X. B. Yu, *J. Alloy. Compd.* **2019**, *794*, 303-324.
- [5] L. Z. Ouyang, W. Chen, J. W. Liu, M. Felderhoff, H. Wang, M. Zhu, *Adv. Energy Mater.* **2017**, *7*, 1700299.
- [6] W. Chen, L. Z. Ouyang, J. W. Liu, X. D. Yao, H. Wang, Z. W. Liu, M. Zhu, *J. Power Sources* **2017**, *359*, 400-407.
- [7] H. I. Schlesinger, H. C. Brown, A. E. Finholt, J. R. Gilbreath, H. R. Hoekstra, E. K. Hyde, *J. Am. Chem. Soc.* **1953**, *75*, 215-219.
- [8] Q. L. Yao, Z. H. Lu, Y. W. Yang, Y. Z. Chen, X. S. Chen, H. L. Jiang, *Nano Res.* **2018**, *11*, 4412-4422.
- [9] Q. L. Yao, Z. H. Lu, W. Huang, X. S. Chen, J. Zhu, *J. Mater. Chem. A* **2016**, *4*, 8579-8583.
- [10] Q. L. Yao, Z. H. Lu, R. Zhang, S. L. Zhang, X. S. Chen, H. L. Jiang, *J. Mater. Chem. A* **2018**, *6*, 4386-4393.
- [11] H. C. Brown, C. A. Brown, *J. Am. Chem. Soc.* **1962**, *84*, 1493-1494.
- [12] Z. M. Huang, A. Su, Y. C. Liu, *Energy* **2013**, *51*, 230-236.
- [13] D. D. Tuan, K. Y. A. Lin, *Chem. Eng. J.* **2018**, *351*, 48-55.
- [14] Y. S. Wei, Y. Wang, L. Wei, X. S. Zhao, X. Y. Zhou, H. T. Liu, *Int. J. Hydrogen Energy* **2018**, *43*, 592-600.
- [15] J. Y. Guo, C. B. Wu, J. F. Zhang, P. X. Yan, J. N. Tian, X. C. Shen, T. T. Isimjan, X. L. Yang, *J. Mater. Chem. A* **2019**, *7*, 8865-8872.
- [16] H. Jia, X. J. Liu, X. Chen, X. X. Guan, X. C. Zheng, P. Liu, *Int. J. Hydrogen Energy* **2017**, *42*, 28425-28433.
- [17] L. Hostert, E. G. C. Neiva, A. J. G. Zarbin, E. S. Orth, *J. Mater. Chem. A* **2018**, *6*, 22226-22233.
- [18] A. Chinnappan, J. M. C. Puguán, W. J. Chung, H. Kim, *J. Power Sources* **2015**, *293*, 429-436.
- [19] G. R. M. Tomboc, A. H. Tamboli, H. Kim, *Energy* **2017**, *121*, 238-245.
- [20] N. Sahiner, F. Seven, *Energy* **2014**, *71*, 170-179.
- [21] T. T. Liu, K. Y. Wang, G. Du, A. M. Asiri, X. P. Sun, *J. Mater. Chem. A* **2016**, *4*, 13053-13057.
- [22] M. Bekiroglu, M. Kaya, C. Saka, *Int. J. Hydrogen Energy* **2019**, *44*, 7262-7275.
- [23] M. X. Ma, L. Wei, F. Jin, *Funct. Mater. Lett.* **2019**, *12*, 1850109.
- [24] M. H. Lee, J. R. Deka, C. J. Cheng, N. F. Lu, D. Saikia, Y. C. Yang, H. M. Kao, *Appl. Surf. Sci.* **2019**, *470*, 764-772.
- [25] B. C. Filiz, A. K. Figen, *Int. J. Hydrogen Energy* **2019**, *44*, 9883-9895.
- [26] Z. T. Gao, C. M. Ding, J. W. Wang, G. Y. Ding, Y. A. Xue, Y. K. Zhang, K. Zhang, P. Liu, X. F. Gao, *Int. J. Hydrogen Energy* **2019**, *44*, 8365-8375.
- [27] B. Chen, S. J. Chen, H. A. Bandal, R. Appiah-Ntiamoah, A. R. Jadhav, H. Kim, *Int. J. Hydrogen Energy* **2018**, *43*, 9296-9306.
- [28] X. Y. Zhang, X. W. Sun, D. Y. Xu, X. M. Tao, P. Dai, Q. J. Guo, X. Liu, *Appl. Surf. Sci.* **2019**, *469*, 764-769.
- [29] R. Edla, S. Gupta, N. Patel, N. Bazzanella, R. Fernandes, D. C. Kothari, A. Miotello, *Appl. Catal. A* **2016**, *515*, 1-9.
- [30] D. Kilinc, O. Sahin, *Int. J. Hydrogen Energy* **2018**, *43*, 10717-10727.
- [31] J. Lee, H. Shin, K. S. Choi, J. Lee, J. Y. Choi, H. K. Yu, *Int. J. Hydrogen Energy* **2019**, *44*, 2943-2950.
- [32] J. Z. Ding, Q. Li, Y. Su, Q. Y. Yue, B. Y. Gao, W. Z. Zhou, *Int. J. Hydrogen Energy* **2018**, *43*, 9978-9987.
- [33] X. C. Shen, Q. Wang, Q. Q. Wu, S. Q. Guo, Z. Y. Zhang, Z. Y. Sun, B. S. Liu, Z. B. Wang, B. Zhao, W. P. Ding, *Energy* **2015**, *90*, 464-474.
- [34] A. Zabielaite, A. Balciunaite, I. Stalnioniene, S. Lichusina, D. Simkunaite, J. Vaiciuniene, B. Simkunaite-Stanyniene, A. Selskis, L. Tamasauskaitė-Tamasiunaite, E. Norkus, *Int. J. Hydrogen Energy* **2018**, *43*, 23310-23318.
- [35] A. Didehban, M. Zabihi, J. R. Shahrouzi, *Int. J. Hydrogen Energy* **2018**, *43*, 20645-20660.
- [36] J. Guo, Y. J. Hou, B. Li, Y. L. Liu, *Int. J. Hydrogen Energy* **2018**, *43*, 15245-15254.
- [37] S. H. Wang, Y. A. Fan, M. Q. Chen, Y. Y. Xie, D. W. Wang, C. Y. Su, *J. Mater. Chem. A* **2015**, *3*, 8250-8255.
- [38] E. Balkanlı, H. E. Figen, *Int. J. Hydrogen Energy* **2019**, *44*, 9959-9969.
- [39] G. Bozkurt, A. Ozer, A. B. Yurtcan, *Int. J. Hydrogen Energy* **2018**, *43*, 22205-22214.
- [40] C. C. Chou, C. H. Hsieh, B. H. Chen, *Energy* **2015**, *90*, 1973-1982.
- [41] H. M. Sun, J. Meng, L. F. Jiao, F. Y. Cheng, J. Chen, *Inorg. Chem. Front.* **2018**, *5*, 760-772.
- [42] S. S. Muir, X. D. Yao, *Int. J. Hydrogen Energy* **2011**, *36*, 5983-5997.
- [43] L. L. Lu, H. J. Zhang, S. W. Zhang, F. L. Li, *Angew. Chem. Int. Ed.* **2015**, *54*, 9328-9332.
- [44] A. Balbay, C. Saka, *Int. J. Hydrogen Energy* **2018**, *43*, 14265-14272.
- [45] A. Balbay, C. Saka, *Int. J. Hydrogen Energy* **2018**, *43*, 21299-21306.
- [46] F. Ali, S. B. Khan, A. M. Asiri, *Int. J. Hydrogen Energy* **2019**, *44*, 4143-4155.
- [47] N. Sahiner, A. O. Yasar, N. Aktas, *Int. J. Hydrogen Energy* **2016**, *41*, 20562-20572.
- [48] N. Sahiner, A. O. Yasar, *Ind. Eng. Chem. Res.* **2016**, *55*, 11245-11252.
- [49] N. Sahiner, S. Demirci, *Int. J. Energy Res.* **2017**, *41*, 736-746.
- [50] N. Sahiner, *Int. J. Hydrogen Energy* **2018**, *43*, 9687-9695.
- [51] N. Sahiner, *J. Power Sources* **2017**, *366*, 178-184.
- [52] A. H. Tamboli, A. R. Jadhav, W. J. Chung, H. Kim, *Energy* **2015**, *93*, 955-962.
- [53] H. K. Cai, L. P. Liu, Q. Chen, P. Lu, J. Dong, *Energy* **2016**, *99*, 129-135.
- [54] F. H. Wang, Y. J. Zhang, Y. A. Wang, Y. M. Luo, Y. N. Chen, H. Zhu, *Int. J. Hydrogen Energy* **2018**, *43*, 8805-8814.
- [55] S. Demirci, A. K. Sunol, N. Sahiner, *Appl. Catal. B: Environ.* **2020**, *261*, 118242.
- [56] S. Demirci, M. Yildiz, E. Inger, N. Sahiner, *Renew. Energy* **2020**, *147*, 69-76.
- [57] B. Ari, M. Ay, A. K. Sunol, N. Sahiner, *Int. J. Energy Res.* **2019**, *43*, 7159-7172.
- [58] N. Sahiner, S. B. Sengel, *Appl. Clay Sci.* **2017**, *146*, 517-525.

Entry for the Table of Contents (Please choose one layout)

Layout 1:

FULL PAPER

Nonmetal catalyst for NaBH_4 hydrolysis is fabricated by covalent modification of silica nanoparticles with protonated poly(ethylene imine). The hydrolysis of 15 mg NaBH_4 catalyzed by 50 mg of the fabricated catalyst could provide a hydrogen generation rate as high as $117.53 \text{ mL min}^{-1} \text{ g}_{\text{cat}}^{-1}$ at $20 \text{ }^\circ\text{C}$. Moreover, the decreased activity of the catalyst after use could be easily restored by regeneration in acetic acid solution.



Lijing Yang, Xiaoshan Huang, Jiapeng Zhang, and Hua Dong*

Page No. – Page No.

Protonated Poly(ethylene imine)-Coated Silica Nanoparticles for Promoting Hydrogen Generation from NaBH_4 Hydrolysis